Alteration of long and short-term hematopoietic stem cell ratio causes myeloid-biased hematopoiesis

Running title; Self-renewal heterogeneity causes myeloid skewing

Katsuyuki Nishi[1,2], Taro Sakamaki[1,2], Akiomi Nagasaka[1,2], Kevin S. Kao[3], Kay Sadaoka[1,2], Masahide Asano[4], Nobuyuki Yamamoto[5], Akifumi Takaori-Kondo[6], Masanori Miyanishi[1,2] *

[1]Hematopoietic Stem Cell Biology and Medical Innovation (HSCBMI), Department of Pediatrics, Kobe University Graduate School of Medicine, Kobe, Hyogo 650-0047, Japan

[2]RIKEN Center for Biosystems Dynamics Research, Kobe, Hyogo 650-0047, Japan

[3]Weill Cornell, Rockefeller, Sloan-Kettering, Tri-Institutional MD-PhD Program, New York, NY

[4]Institute of Laboratory Animals, Kyoto University Graduate School of Medicine, Kyoto, Kyoto, 606-8501, Japan.

[5]Department of Pediatrics, Kobe University Graduate School of Medicine, Kobe, Hyogo 650-0017, Japan

[6]Department of Hematology and Oncology, Kyoto University Graduate School of Medicine, Kyoto, Kyoto 606-8507, Japan

*Correspondence: Masanori Miyanishi, M.D, Ph.D.

Hematopoietic Stem Cell Biology and Medical Innovation (HSCBMI), Department of Pediatrics, Kobe University Graduate School of Medicine, Kobe, Hyogo 650-0047, Japan

E-mail: miya75@med.kobe-u.ac.jp

Phone: 078-304-6037

FAX: 078-304-6100

Abstract

Myeloid-biased hematopoiesis is a well-known age-related alteration. Several possibilities, including myeloid-biased hematopoietic stem cell (HSC) clones, may explain this. However, the precise mechanisms remain controversial.

Utilizing the Hoxb5 reporter system to prospectively isolate long-term HSCs (LT-HSCs) and short-term HSCs (ST-HSCs), we found that young and aged LT-HSCs co-transplanted into the same recipients demonstrated nearly equivalent myeloid lineage output, contrary to the theory of myeloid-biased HSC clones. Transcriptomics indicated no significant myeloid gene enrichment in aged LT-HSCs compared to their young counterparts. Instead, transplanting reconstituted young HSCs with the ratio of LT/ST-HSCs seen in aged mice can significantly skew the lineage output to myeloid cells. In addition, while the niche environment in the bone marrow minimally affects myeloid-biased hematopoiesis, aged thymi and spleens substantially hinder lymphoid hematopoiesis, resulting in further myeloid-domination. Thus, we demonstrate that myeloid-biased hematopoiesis in aged organisms originates due to alteration of the ratio between LT-HSCs and ST-HSCs rather than in heterogeneous HSC clones with various cell fates.

Introduction

Age-associated changes in individuals are deeply correlated with progressive attenuation of cellular functions in tissue stem cells of organs (Jones and Rando 2011). In the hematopoietic system, hematopoietic stem cells (HSCs), which possess self-renewal capacity and multipotency (Spangrude et al., 1988; Weissman and Shizuru 2008; Majeti et al., 2007), are responsible for various hematopoietic alterations with age, such as reduced self-renewal capacity (Morrison et al., 1996) and myeloid-biased hematopoiesis (Muller-Sieburg et al., 2004; Challen et al., 2010) due to their functional decline. For example, myeloid-biased hematopoiesis potentially reduces response to infections (Webster, 2000), reduces vaccination efficacy (Crooke et al., 2019), and increases myeloid malignancy (Rossi et al., 2008) in aged individuals. To comprehend these age-associated physiological changes, myeloid-biased hematopoiesis has been studied in considerable detail.

Based on the experimental observation that transplantation of aged HSCs exhibits more myeloid-biased differentiation in young recipient mice than transplantation of young HSCs, this phenotype has been thought to originate in cell-intrinsic changes in the HSC compartment (Geiger et al., 2013; De Haan and Lazare 2018; Schultz and Sinclair 2016). A myeloid-biased phenotype after aged HSC transplantation leads to the suggestion that myeloid-biased HSC clones selectively expand with age (Cho et al., 2008; Pang et al., 2011). Transcriptome and epigenetic analyses showing that a set of genes related to myeloid differentiation is significantly enriched in aged HSCs compared to young HSCs (Rossi et al., 2005; Grover et al., 2016) further supports this hypothesis.

On the other hand, some reports support a different point of view in light of experimental evidence showing that aged lymphoid-biased HSCs still demonstrate the same level of

lymphopoiesis as their younger counterparts, despite exhibiting a myeloid-biased gene expression pattern (Montecino-Rodriguez et al., 2019). This result highlights the limitations of predicting a pattern of HSC differentiation based upon gene expression patterns. Moreover, myeloid progenitors such as granulocyte-macrophage progenitor (GMP) and common myeloid progenitor (CMP) should also increase with age if the selective expansion of myeloid-biased HSCs leads to an increase of myeloid cells in peripheral blood (PB). However, increment of such progenitors with age was not consistently demonstrated in earlier research (Rossi et al., 2005; Nilsson et al., 2016; Min et al., 2006). Additionally, a mathematical model demonstrated that aging had no effect on the daily production of CMP supplied from multipotent progenitors (MPP) (Busch et al., 2015; Dorshkind et al., 2020).

As such, while selective expansion of myeloid-biased HSC clones is the most widely accepted hypothesis to explain myeloid-biased hematopoiesis in aging (Mejia-Ramirez and Florian, 2020; SanMiguel et al., 2020), other mechanisms may exist in light of the inconsistent cellular behavior of progenitor fractions relative to HSCs. To the best of our knowledge, no reports have analyzed kinetics of age-associated changes in HSCs, progenitors, and PB cells simultaneously. Therefore, we started our investigation by examining the correlation between age-related changes in PB and BM to shed light on the mechanism underlying myeloid-biased hematopoiesis that occurs during aging.

Results

The discrepancy of age-associated alternation in peripheral blood and bone marrow calls into question the existence of a myeloid-biased clone

Mouse HSC research on aging has used mice aged 18 months or older (Challen et al., 2010; Cho et al., 2008; D. J. Rossi et al., 2005; Grover et al., 2016; Montecino-Rodriguez et al., 2019; Nilsson et al., 2016). However, given that continuous accumulation of cellular stress with age causes a gradual decline of cellular functions, a comprehensive analysis from young to old mice is necessary to unravel mechanisms by which age-associated, myeloid-biased hematopoiesis progress. Hence, we analyzed changes in PB (**Fig. S1 A**) at multiple time points from young to old mice. These results showed that the percentage of myeloid cells began to change as early as 6 months in mice and continued to increase at a constant rate until the age of ≥ 23 months (**Fig. 1 A**).

It has been reported that myeloid-biased hematopoiesis is caused by a selective increase of myeloid-biased clones in the immunophenotypically defined (surface-antigen defined) HSC fraction (**Fig. S1 B**) (Beerman et al., 2010). According to this hypothesis, age-associated myeloid hematopoiesis progression in PB would be paralleled by an increase in myeloid-biased HSC clones. Therefore, we examined the frequency of the HSC and progenitor fractions in the BM at multiple time points (**Fig. S1, B and C**). We found that the frequency of immunophenotypically defined HSC in BM rapidly increased up to the age of 12 months. After the age, they remained plateaued throughout the observation period (**Fig. 1 B**). On the other hand, in contrast to what we anticipated, the frequency of GMP was stable, and the percentage of CMP actually decreased significantly with age, defying our prediction that the frequency of components of the myeloid differentiation pathway, such as CMP, GMP, and MEP would increase in aged mice if myeloid-biased HSC clones increase with age (**Fig. 1 B**).

Finally, we determined the ratio of each fraction in young mice versus aged mice to compare the age-associated transition pattern of components comprising the myeloid

differentiation pathway. This analysis revealed that age-associated transition patterns of immunophenotypically defined HSC and CMP in BM were not paralleled with myeloid cell in PB (**Fig. 1 C**). These findings called into question the hypothesis that there is a selective increase of myeloid-biased HSC clones in the aged BM. We then set out to elucidate the mechanism by which myeloid-biased phenotypes arise in the PB of aged mice.

The long-term observation of 2-year-old LT-HSC's differentiation does not indicate the expansion of myeloid-biased clones.

Numerous studies have claimed that the myeloid-skewed phenotype observed in PB of aged mice is caused by myeloid-biased HSC clones selectively expanded from HSCs with originally heterogeneous differentiation potentials (Beerman et al., 2010; Dykstra et al., 2011; Sudo et al., 2000). Other studies have reported that immunophenotypically defined HSCs possess heterogeneity associated with self-renewal capacity, suggesting the existence of at least two different populations in the HSC compartment, LT-HSCs and ST-HSCs (Morrison and Weissman 1994; Spangrude et al., 1995). Since LT-HSCs have extensive self-renewal capacity, while ST-HSCs lose their self-renewal capacity within a short period, LT-HSCs are thought to persist in the BM throughout life and to enrich age-associated changes compared to ST-HSCs. Therefore, we expect that LT-HSC-specific analyses will help to answer whether myeloid-biased HSC clones exist.

We previously reported that Hoxb5 exclusively marks LT-HSCs in young mice (Chen et al., 2016). However, we have not tested in aged mice whether Hoxb5 specifically labels LT-HSCs and helps to distinguish LT-HSCs and ST-HSCs from immunophenotypically defined HSCs (hereafter, bulk-HSCs). To confirm this, we first analyzed expression of

Hoxb5 in bulk-HSC, MPP, Flk2$^+$, and Lin$^-$Sca1$^-$c-Kit$^+$ populations in aged *Hoxb5*-tri-mCherry mice. We observed that Hoxb5 was exclusively expressed in bulk-HSCs (**Fig. 2 A**). Then, to verify long-term engraftment, we conducted a transplantation assay utilizing Hoxb5$^+$ HSCs and Hoxb5$^-$ HSCs, respectively, isolated from 2-year-old mice (**Fig. 2 B**). We observed that only recipients receiving aged Hoxb5$^+$ HSCs exhibited continuous hematopoiesis 16 weeks after primary transplantation (**Fig. 2, C and E; Fig. S2 A**). In secondary transplantation analysis, only recipients receiving Hoxb5$^+$ HSCs exhibited robust hematopoiesis throughout the period of observation, indicating that Hoxb5 can be used as a specific marker of LT-HSCs in aged mice, as well as young mice (**Fig. 2, D and F; Fig. S2 B**).

A serial transplantation assay with a period of observation longer than 8 months should be long enough to observe further myeloid-biased change. If bulk-HSCs isolated from aged mice are already enriched by myeloid-biased HSC clones, we should see more myeloid-biased phenotypes 16 weeks after primary and the secondary transplantation. However, we found that kinetics of the proportion of myeloid cells in PB were similar across primary and the secondary transplantation and that the proportion of myeloid cells gradually decreased over time (**Fig. 2 G**). These results suggest the following two possibilities: either myeloid-biased HSCs do not expand in the LT-HSC fraction, or the expansion of myeloid-biased clones in 2-year-old mice has already peaked.

Direct comparison between young vs. aged LT-HSC differentiation reveals that LT-HSCs exhibit unchanged lineage output throughout life

We developed a co-transplantation assay to directly compare the differentiation capacity between young and aged LT-HSCs by co-transplanting ten young GFP$^+$ LT-HSCs and

ten aged GFP$^-$ LT-HSCs into the same recipient mice (**Fig. 3 A**). Then, we found that the myeloid lineage proportions from young and aged LT-HSCs were nearly comparable during the observation period after transplantation (**Fig. 3, B and C**). Furthermore, by analyzing the proportion of mature cell types derived from young and aged LT-HSCs in the same donor, we directly compared the capacity for hematopoietic reconstitution in each mature cell type between young and aged LT-HSCs. We confirmed again that the reconstitution ratio was almost the same across all lineages, although bulk hematopoiesis derived from young LT-HSCs predominated (**Fig. 3 D**). These results indicate that the differentiation potential of LT-HSCs remains unchanged throughout their lives.

Several reports have demonstrated that transplanting mixed/bulk-HSCs—a combination of LT-HSCs and ST-HSCs—obtained from old animals results in blatantly myeloid-biased hematopoiesis (Beerman et al., 2010; Dykstra et al., 2011; Sudo et al., 2000). To test this, we co-transplanted bulk-HSCs from young and old mice to corroborate this (**Fig. S3 A**). As previously described, we observed that aged bulk-HSC exhibited a myeloid-skewed phenotype (**Fig. S3 B and C**). Additionally, we observed that aged bulk-HSC reconstitution exhibited higher reconstitution of myeloid cells compared to young bulk-HSCs (**Fig. S3 D**). These findings unmistakably demonstrated that mixed/bulk-HSCs showed myeloid skewed hematopoiesis in PB with aging, while LT-HSCs exhibited unchanged lineage output throughout life.

LT-HSCs never show myeloid-related gene set enrichment during aging

Although the results of co-transplantation of young and aged LT-HSCs did not demonstrate lineage-biased output by LT-HSCs throughout life, enrichment of myeloid genes in aged bulk-HSCs shown by previous studies supports the idea that myeloid-

208 biased hematopoiesis is caused by selective expansion of myeloid-biased HSC clones (D.
209 J. Rossi et al., 2005; Grover et al., 2016). To compare age-associated myeloid gene
210 enrichment, we isolated bulk-HSC, LT-HSCs, and ST-HSCs from young or aged mice
211 (**Fig. 4 A**).
212 To ensure the quality of the sorted fraction for subsequent RNA-seq analyses, we verified
213 the Hoxb5 read counts (**Fig. S4 A**). Cluster dendrograms using the whole transcriptome
214 confirmed that cell fractions isolated from young and aged mice clustered into distinct
215 groups (**Fig. 4 B**). Then, using sets of aging-related genes, such as inflammation
216 (Liberzon et al., 2015; Pietras 2017), DNA damage (p53 pathway) (Liberzon et al., 2015;
217 D. J. Rossi et al., 2007), cell cycle progression (E2F target) (Liberzon et al., 2015;
218 Kowalczyk et al., 2015), and a common aging signature (Flohr Svendsen et al., 2021), we
219 ran a violin plot analysis on each cell fraction to confirm the occurrence of typical aging-
220 related gene expression changes. We found age-associated changes in inflammation and
221 the DNA damage between cells isolated from young and aged mice, but very similar
222 patterns regardless of cell fraction in young or aged mice. In terms of cell cycle
223 progression and aging signature genes, however, we discovered that only the young LT-
224 HSC fraction differed from other young fractions and tended to represent similar gene
225 expression pattern with aged fractions (**Fig. 4 C**). Then, taking LT-HSC specific gene
226 expression pattern into account, we looked at expression patterns of specific genes that
227 had been highly validated by experiments as being associated with myeloid-biased HSC
228 (Beerman et al., 2010; Flohr Svendsen et al., 2021; Sanjuan-Pla et al., 2013; Mann et al.,
229 2018). We discovered that expression of these genes is relatively comparable between
230 young and aged LT-HSCs, but not other fractions (**Fig. S4 B**).

231 A recent comprehensive analysis of mouse HSC aging using multiple RNAseq data sets
232 claimed that almost 80% of differentially expressed genes are poorly reproducible across
233 data sets (Flohr Svendsen et al., 2021). In fact, we found that almost 80% of genes are
234 not shared when we compare three representative myeloid/lymphoid gene sets (Sanjuan-
235 Pla et al., 2013; Chambers et al., 2007; Pronk et al., 2007). Additionally, most genes were
236 only used in a single gene set (**Fig. 4, D and E**). By using only genes that were shared in
237 these gene sets, we ran a gene set enrichment analysis (GSEA) to see whether
238 myeloid/lymphoid genes were enriched in aged LT-HSCs or other fractions. Neither aged
239 LT-HSC nor aged ST-HSC exhibited myeloid/lymphoid gene enrichment, while shared
240 myeloid-related genes tended to be enriched in aged bulk-HSCs (**Fig. 4, F and G**). On
241 the other hand, GSEA analysis using original gene sets, respectively, showed inconsistent
242 results (**Fig. S4, C and D**).
243
244 ***A myeloid-biased phenotype in peripheral blood depends on the relative decrease of***
245 ***ST-HSC in the HSC compartment with age***
246 While transplantation of aged bulk-HSCs exhibits a myeloid-biased phenotype in PB
247 shown in previous reports (Beerman et al., 2010; Dykstra et al., 2011; Sudo et al., 2000)
248 and our results (**Fig. S3**), aged LT-HSCs remain stable in terms of the balance of their
249 differentiation potential between myeloid and lymphoid production (**Fig. 3**). Comparative
250 transcriptome analyses demonstrated that neither LT-HSCs nor ST-HSCs, which are
251 functionally more homogeneous than bulk-HSCs, exhibited myeloid gene set enrichment
252 with age, whereas aged bulk-HSCs tended to show more myeloid gene set enrichment
253 than their young counterparts (**Fig. 4**). We then tried to figure out what causes the
254 myeloid-biased phenotype in PB after transplantation of bulk-HSCs.

Because LT-HSCs in bulk-HSCs exhibit nearly constant level of hematopoiesis throughout life, we hypothesized that ST-HSCs could be the key to discovering mechanisms underlying the myeloid-skewing phenomenon. First, we revisited our previous study (Chen et al., 2016), which demonstrated that transplanted ST-HSCs maintain lymphocyte production while rapidly losing myeloid lineage production in recipients. This result may potentially indicate the presence of HSC clones with a preference for lymphoid differentiation. Given that donor cells obtained from primary recipients receiving ST-HSCs do not undergo hematopoiesis in secondary transplantation (Chen et al., 2016), it is likely that all ST-HSCs have already lost their ability to self-renew and have disappeared from the HSC fraction in primary recipients. To confirm this, we transplanted ten LT-HSCs or ST-HSCs and then analyzed PB and BM (**Fig. 5 A**). As we previously reported (Chen et al., 2016), donor-derived hematopoiesis eventually becomes lymphocyte-dominant in PB of ST-HSC recipients over time (**Fig. 5 B**). Subsequently, it was determined that the vast majority of T cell subsets are memory cells (**Fig. 5, C and D**). In addition, unlike recipients receiving LT-HSCs, recipients receiving ST-HSCs lacked any bulk-HSCs in their BM (**Fig. 5, E and F**). These results strongly suggest that lymphoid-biased hematopoiesis observed after transplantation of ST-HSCs is due to persistence of memory-type lymphocytes in PB, rather than to *de novo* lymphopoiesis from lymphoid-biased HSC clones. Persistence of memory-type lymphocytes from ST-HSCs may have led us to misinterpret mechanisms underlying myeloid-biased hematopoiesis after aged bulk-HSC transplantation. To verify this hypothesis, we examined kinetics of the LT-HSC/ST-HSC ratio in the bulk-HSC population, revealing the ratio of ST-HSC to LT-HSC decreased with age (**Figure S5**).

Thus, we hypothesized that the relative decrease in the ST-HSC ratio in the aged bulk-HSC fraction would lead to reduction of memory-type lymphocytes and myeloid-biased hematopoiesis following transplantation of aged bulk-HSCs. To test this hypothesis, we isolated LT-HSCs and ST-HSCs from young donor mice and reconstituted them with a 2:8 ratio (as in young mice) or a 5:5 ratio (as in aged mice) prior to transplanting them (**Fig. 6 A**). Four weeks after transplantation, PB analysis revealed that both groups had comparable patterns of hematopoiesis. In contrast, recipient mice transplanted with a 5:5 ratio began to exhibit more myeloid-biased hematopoiesis eight weeks after transplantation, and by week 16, they produced significantly more myeloid cells than the other group (**Fig. 6, B-D**). Additionally, we conducted further investigations to determine whether lymphoid hematopoiesis could be accelerated by alteration of LT-HSC/ST-HSC ratios using cells from aged mice. To verify this, we isolated aged LT-HSCs and ST-HSCs and reconstituted them with a 5:5 ratio or a 2:8 ratio prior to transplantation (**Fig. S6 A**). Peripheral blood analysis revealed that lymphoid lineage output in the recipient mice transplanted with a 2:8 ratio was significantly greater than those with a 5:5 ratio (**Fig. S6 B-D**). Based on these findings, we concluded that myeloid-biased hematopoiesis observed following transplantation of aged HSCs was caused by a relative decrease in ST-HSC in the bulk-HSC compartment in aged mice rather than the selective expansion of myeloid-biased HSC clones.

Age-associated extramedullary changes accelerate myeloid-biased hematopoiesis

We found that the fluctuating LT-HSC/ST-HSC ratio in the bulk-HSC compartment corresponded with the myeloid-biased hematopoiesis associated with aging. In contrast, the degree of myeloid bias observed in mice older than 23 months without transplantation

(**Fig. 1 A**; 49.0 ± 23.4%) was significantly greater than in recipient mice receiving young mixed HSCs with a 5:5 ratio 16 weeks after transplantation (**Fig. 6 D;** 30.8 ± 30.8%). This difference indicated that other intrinsic or extrinsic factors might exist in mice older than 23 months to promote myeloid-biased hematopoiesis. To investigate this further, we transplanted ten GFP^+ young LT-HSCs into young or 2-year-old recipient mice and examined their PB (**Fig. 7 A**). We limited the observation period to 12 weeks because many aged recipient mice had died prior to that point (**Fig. 7 B**). PB analysis revealed that aged recipient mice receiving young LT-HSCs produced significantly more myeloid cells than young recipient mice (**Fig. 7, C-E**). These results suggested that recipient-dependent extrinsic factors, rather than intrinsic factors of transplanted HSCs, had a greater impact on hematopoietic cell differentiation. Then, we examined BM to determine what extrinsic factors affected differentiation of transplanted HSCs. Percentages of CMP and GMP, downstream components of myeloid differentiation, were stable or significantly lower in aged recipient mice than in young recipient mice, just as they were in non-treated aged mice (**Fig. 7 F; Fig. 1 B**). In addition, the percentage of CLP, a downstream component of lymphoid differentiation, did not differ between young and aged recipients (**Fig. 7 F**). In contrast to previous studies (Pinho et al., 2018; Ergen et al., 2012), these findings suggested that intramedullary age-associated changes may not have a significant impact on LT-HSC differentiation.

Thymi and spleens of recipient mice were then examined, as these are the structures of lymphoid maturation and production of lymphoid progenitors following migration from BM and prior to their appearance in PB. Donor cells were not microscopically detectable in the majority of aged recipient mice (**Fig. 7, G and I**), and quantitative analysis using a flow cytometer revealed that the frequency of donor cells in spleens and thymi of aged

recipients was significantly lower than in young recipients (**Fig. 7, H and J**). These results indicated that the process of lymphoid lineage differentiation was impaired in the spleens and thymi of aged mice compared to young mice, resulting in enhanced myeloid-biased hematopoiesis in PB due to a decrease in the *de novo* lymphocyte production.

Discussion

Age-related, myeloid-biased hematopoiesis has been suggested as a potential reason for the decline in acquired immunity in the elderly (Geiger et al., 2013). This process has been linked to an increase in myeloid-biased HSC clones in the bulk-HSC fraction identified by surface antigens through aging. By isolating LT-HSCs and ST-HSCs, respectively, we discovered that age-related changes in the ratio of ST-HSCs to LT-HSCs in bulk-HSCs is responsible for myeloid-biased hematopoiesis.

When aged bulk-HSCs were transplanted into young mice, post-transplant hematopoiesis in recipient mice was significantly biased toward myeloid in PB compared to transplantation of young bulk-HSCs (Beerman et al., 2010; Dykstra et al., 2011; Sudo et al., 2000). Historically, this myeloid-biased hematopoiesis derived from aged bulk-HSCs has been considered as evidence supporting expansion of myeloid-biased HSC clones with aging (Geiger et al., 2013; de Haan and Lazare 2018). Other studies, however, suggest that blockage of lymphoid hematopoiesis in aged mice results in myeloid-skewed hematopoiesis through alternative mechanisms (Montecino-Rodriguez et al., 2019). To clarify the cause for this disparity, we chose to examine the LT-HSC fraction, which persists in the BM for long periods of time and is enriched for aging-related alterations. We discovered that post-transplant hematopoiesis of aged LT-HSCs did not vary from that of young LT-HSCs in terms of differentiation capacity. Expression of myeloid-

related genes was not significantly altered when LT-HSCs from young and aged mice were compared. Therefore, we inferred that age-related myeloid-biased hematopoiesis cannot be attributed to an increase in myeloid-biased HSCs, at least among LT-HSCs. Given that bulk-HSCs consist of LT-HSCs and ST-HSCs, and that LT-HSCs exhibit no change in differentiation potential with age, we hypothesized that ST-HSCs may be responsible for the myeloid-skewing phenotype in PB. Transcriptomic analysis revealed no enrichment of myeloid-related genes in the ST-HSC fraction, ruling out the possibility of an increase in myeloid-biased HSCs in the ST-HSC fraction. Alternatively, we observed a proportionate decrease in ST-HSCs in bulk-HSCs accompanying an increase in LT-HSCs. We postulated that this relative decrease in ST-HSC ratio is responsible for myeloid-biased hematopoiesis. When isolated LT-HSCs and ST-HSCs from young mice were reconstituted to replicate an aged BM type in terms of the LT-HSC/ST-HSC ratio, we discovered that PB was strongly skewed towards myeloid cells after transplantation of reconstituted HSCs. In contrast, transplantation of reconstituted HSCs with a young BM type resulted in a significantly lymphoid-skewed PB profile.

On the other hand, it has been reported that myeloid-biased HSCs have a more persistent capacity for self-renewal (Muller-Sieburg et al., 2004). In fact, in our prior investigation comparing PB 16 weeks post-transplant, myeloid cell production in PB was greater when LT-HSCs were transplanted, while ST-HSC transplantation resulted in a considerable increase in lymphoid cell production (Chen et al., 2016). It is therefore possible that the LT-HSCs and ST-HSCs we isolated utilizing the Hoxb5 reporter system are myeloid- and lymphoid-biased HSCs, respectively. However, the myeloid-producing capacity of LT-HSCs and ST-HSCs 4 weeks post-transplantation is equivalent (Chen et al., 2016). In contrast, 16 weeks after transplantation, ST-HSC transplant recipients demonstrate

374 negligible myeloid development and a predominance of lymphocytes, unlike LT-HSC
375 transplant recipients (Chen et al., 2016). These characteristics show that early post-
376 transplant ST-HSCs lack the phenotypic of lymphoid-biased HSCs. When ST-HSC-
377 transplanted BM cells are employed as donors for secondary transplantation, no donor-
378 cell-derived hematopoiesis is detected in recipients (Chen et al., 2016). In addition, HSCs
379 are not observed in the BM following transplantation of ST-HSCs (**Fig. 5**). These results
380 indicate that ST-HSCs lose their capacity for self-renewal earlier after transplantation
381 than LT-HSCs. In addition, phenotypic examination of lymphocytes in PB after ST-HSC
382 transplantation revealed that nearly all of them were memory cells, and that there was no
383 *de novo* supply of T cells. In other words, ST-HSCs may have been erroneously classified
384 as lymphoid-biased HSCs due to the preservation of memory lymphocytes with a long
385 half-life in the peripheral circulation, despite the absence of *de novo* hematopoiesis
386 following transplantation of ST-HSCs. These findings suggest that the bias toward
387 myeloid and lymphoid lineages in post-transplant PB is not regulated by heterogeneity of
388 multipotency, but by heterogeneity of self-renewal capacity.
389 Multiple extrinsic factors have been implicated as HSC-independent causes of myeloid-
390 biased hematopoiesis associated with aging. Some findings suggest that cell interaction
391 with niche cells in BM is altered (Pinho et al., 2018), whereas others claim that chronic
392 inflammation in aged mice lowers production of lymphoid progenitors and induces
393 myeloid-biased hematopoiesis (Montecino-Rodriguez et al., 2019; Ergen et al., 2012). To
394 identify HSC-independent causes of myeloid-biased hematopoiesis specifically, we
395 transplanted young LT-HSCs into young or aged mice. Cellular differentiation observed
396 in BM revealed that proportions of GMP, MEP, and CLP are unchanged between young
397 and aged recipients. In contrast, an examination of spleens and thymi, the sites of

lymphocyte maturation, revealed the absence of donor cells in aged recipients. These findings suggest that myeloid cells increase in aging mice due to a relative decrease in the ratio of mature lymphocytes in PB, resulting from inhibition of lymphocyte maturation outside the BM, such as in the thymus and spleen, rather than a significant change in cell differentiation caused by the intramedullary environment. Attempts have been made in the past to restore thymus function in aged mice by administering keratinocyte growth factor (KGF) (S. W. Rossi et al., 2007). Indeed, in aged mice, lymphocyte hematopoiesis recovers, which is consistent with our results that the extramedullary environment influences the myeloid-bias phenotype in PB (S. W. Rossi et al., 2007).

It has been clinically documented that recovery of the lymphocyte fraction in PB is delayed in elderly donors, compared to young donors (González-Vicent et al., 2017; Baron et al., 2006). Although it is undeniable that this phenomenon may be due to decreased HSC hematopoietic potential, it may also be due to a change in the ratio of LT-HSC/ST-HSCs in bulk-HSCs, as described in our report, which may give the appearance of a myeloid bias in PB after transplantation. It has also been noted that lymphocyte recovery is delayed in elderly patients compared to younger patients (Berger et al., 2008; van der Maas et al., 2021). Age-related loss in thymus and spleen functions has been recorded in humans, implying that the same mechanism is acting as in our mouse observations. If it is possible to assess and regulate the LT-HSC/ST-HSC ratio in donors and thymus/spleen function in recipients in the future, it will help to develop accurate models for predicting lymphocyte recovery after transplantation as well as new transplantation strategies.

In summary, we have demonstrated for the first time that the ratio of LT-HSC/ST-HSC is important in age-related myeloid skewed hematopoiesis as an HSC-dependent factor and that aging-related thymus and spleen dysfunction also contributes significantly as an HSC-independent factor. Furthermore, here we propose a "self-renewal heterogeneity model" as a new mechanism for hematopoietic heterogeneity, including myeloid-biased hematopoiesis in aged mice (**Fig. 8**). In addition to this report, we have also shown that cellular differentiation in the PB after transplantation can vary by changing transplantation conditions, ultimately altering self-renewal ability (Sakamaki et al., 2021; Nishi et al., 2022). This highlights the significance of deciphering molecular processes that regulate the heterogeneity of HSC self-renewal capacity, which will help to provide a better understanding of the hematopoietic system and the hematopoietic hierarchy in the future.

Methods

Mice

Mice with an *Hoxb5*-tri-mCherry (C57BL/6J background), derived from our previous work (Chen et al., 2016), were harvested for donor cells for transplantation, PB, and BM analysis. CAG-EGFP mice (C57BL/6J background) were bred with *Hoxb5*-tri-mCherry for transplantation experiments. 8-14-week-old C57BL/6-Ly5.1 mice (purchased from Sankyo Labo Service) were used as recipients for transplantation assays. For aged recipients, 2-year-old CD45.2 C57BL/6J mice were purchased from CLEA Japan. Supporting BM cells were collected from 8-12-week-old C57BL/6-Ly5.1 × C57BL/6J (F_1 mice $CD45.1^+/CD45.2^+$). All mice were housed in specific pathogen-free (SPF) conditions and were carefully observed by staff members. Mice were bred according to

RIKEN or Kyoto University. All animal protocols were approved by the RIKEN Center for Biosystems Dynamics Research and Kyoto University.

Flow cytometry, cell sorting, and bone marrow analyses

Flow cytometry and cell sorting were performed on a FACS Aria II cell sorter (BD Biosciences) and analyzed using FlowJo™ software (BD Biosciences). Bone marrow (BM) cells were collected from bilateral tibias, femurs, humeri, and pelvises in Ca^{2+}- and Mg^{2+}-free PBS supplemented with 2% heat-inactivated bovine serum (Gibco) and 2 mM EDTA (Thermo Fisher Scientific). Cells were passed through 100-μm, and 40-μm strainers (Corning) before analysis and sorting. Prior to staining, samples were blocked with 50 ug/mL rat IgG (Sigma-Aldrich) for 15 min. To enrich HSCs and progenitor populations for sorting and bone marrow analyses, cells were stained with APC-eFluor780-conjugated anti-c-Kit (clone: 2B8) and fractionated using anti-APC magnetic beads and LS columns (both Miltenyi Biotec). c-Kit^{+} cells were then stained with combinations of antibodies as described in Supplemental Table 1. All staining was incubated at 4°C for 30 min, except for CD34 staining, which was incubated for 90 min. Samples were washed twice after staining. Prior to flow cytometry or cell sorting, samples were stained with SYTOX Red Dead Cell Stain (Life Technologies) or 7-aminoactinomycin D (BioLegend). Cells were double sorted for purity.

Transplantation and peripheral blood analyses

12-24 hours prior to transplantation, C57BL/6-Ly5.1 mice, or aged C57BL/6J recipient mice were lethally irradiated with single doses of 8.7 Gy or 9.1Gy. For transplantation assays, donor cells were first combined with 2×10^5 whole bone marrow supporting cells

(C57BL/6-Ly5.1 × C57BL/6J F_1 mice CD45.1$^+$/CD45.2$^+$) in 200 μL of PBS with 2% FBS, and then injected into the retro-orbital venous plexus. For evaluation of post-transplant kinetics, PB was collected and analyzed. At each time point, 50 μL of blood were collected from the tail vein and re-suspended in Ca^{2+}- and Mg^{2+}-free PBS supplemented with 2 mM EDTA. Red blood cells were lysed twice on ice for 3 min with BD Pharm Lyse Buffer (BD Pharmingen). Identification of leukocyte subsets was performed by staining with antibodies. Antibody information was described in Supplemental Table 1. For evaluation of lineage output, the frequency of each lineage (NK cell, B cell, T cell, neutrophil, and monocyte) was determined in the whole fraction. The analysis of donor lineage output was restricted to donor cells showing ≥ 0.1% donor chimerism at the last PB analysis to allow reliable detection. The percentage of donor chimerism in PB was defined as the percentage of CD45.1$^-$CD45.2$^+$ cells among total CD45.1$^-$CD45.2$^+$ and CD45.1$^+$CD45.2$^+$ cells. PB data represents mice which survived until the last PB analysis.

Thymus and Spleen analysis

Thymi and spleens were harvested and disrupted into a single cell suspension. Cells were passed through 100-μm, and 40-μm strainers (Corning). Isolated thymocytes and splenocytes were incubated on ice for 30 min with appropriately diluted antibodies in staining buffer. Identification of B cells in spleens and T cells in thymi was performed by staining with antibodies described in Supplemental Table 1. Prior to flow cytometry or cell sorting, samples were stained with SYTOX Red Dead Cell Stain (Life Technologies).

493 **Tissue imaging**

494 Freshly dissected spleens and thymi were fixed in 4% PFA (Nacalai tesque) in PBS for
495 24 h at 4°C. After PFA washout with PBS, tissues were cryoprotected with 30% sucrose
496 in PBS for 24 h at 4°C, embedded in Tissue-Tek O.C.T. compound (Sakura Finetek), and
497 snap-frozen in liquid nitrogen. Serial 10-μm longitudinal cryostat sections were obtained
498 using CryoStar NX50 (Thermo Fisher Scientific). Cell nuclei were counterstained with
499 4',6-diamidino-2-phenylindole (DAPI, 1 μg/mL, Roche). To reduce autofluorescence,
500 tissue sections were treated with Vector TrueVIEW autofluorescence quenching kit
501 (Vector Laboratories). Images were obtained from Leica TCS SP8 (Leica).
502
503 **RNA sequencing**
504 Total RNA was isolated with Trizol (Thermo Fisher Scientific) and cleaned up using
505 RNeasy MinElute columns (QIAGEN). cDNA libraries were prepared from bulk-HSCs,
506 ST-HSCs and LT-HSCs using a KAPA RNA HyperPrep kit with RiboErase (HMR)
507 (Kapa Biosystems) and sequenced using a Hiseq 1500 (Illumina) to obtain 2 × 127 base-
508 pair (bp) paired-end reads. Three replicates were sequenced for each population. Raw
509 transcriptome sequence data were mapped to the genome (mm10) using HISAT2 (ver
510 2.1.0) (Kim et al., 2015). Alignments were then passed to StringTie (ver 1.3.4d), which
511 was used to assemble and quantify transcripts in each sample (Pertea et al., 2016). EdgeR
512 (ver 3.22.5) was then used to compare all transcripts across conditions and to produce
513 tables and plots of differentially expressed genes and transcripts (Robinson et al., 2009).
514 Normalization with the TMM method was performed with the edgeR package in
515 Bioconductor (https://bioconductor.org/). Genes (12,808 genes) were selected for
516 hierarchical clustering based on the mean of TMM normalized read counts across all

517 samples' cells (mean ≥ 1). Then, clustering was performed by using the hclust function
518 for R (distance = Spearman's correlation'; method = 'ward.D2'). We depicted Venn
519 diagrams and performed GSEA analyses in Figures 4D-G and S4C-D using previously
520 published gene sets after excluding genes that could not be annotated by our
521 transcriptome dataset. GSEA was performed using GSEA software
522 (http://www.broadinstitute.org/gsea) with default settings (Subramanian et al., 2005).
523

524 **Quantification and statistical analyses**

525 Statistical analyses were performed using ggplot2 in R (version 4.1.2) or Microsoft Excel.
526 Sample size for each experiment and replicate numbers of experiments are included in
527 figure legends. Statistical significance was determined using Welch's t test. *P* values <
528 0.05 were considered significant.
529

530 **Data and materials availability**

531 Sequencing data has been deposited in the Gene Expression Omnibus under accession
532 code GSE226803. Correspondence and requests for materials should be addressed to
533 M.M. (miya75@med.kobe-u.ac.jp).
534

535 **Acknowledgements**

536 We gratefully acknowledge Hiroshi Kiyonari for animal care and providing recipient
537 mice at RIKEN BDR. Shigehiro Kuraku, Mitsutaka Kadota, and Chiharu Tanegashima
538 provided technical support for RNA sequencing and analysis at RIKEN BDR. Momo
539 Fujii performed imaging experiments at RIKEN BDR. Hitomi Oga, Kayoko Nagasaka,
540 and Masaki Miyahashi provided laboratory management at Kobe University. The authors

gratefully acknowledge ongoing support for this work: Masanori Miyanishi was supported by the Japan Society for the Promotion of Science (JSPS) KAKENHI Grant Number JP17K07407 and JP20H03268, The Mochida Memorial Foundation for Medical and Pharmaceutical Research, The Life Science Foundation of Japan, The Takeda Science Foundation, The Astellas Foundation for Research on Metabolic Disorders, AMED-PRIME, AMED under Grant Number JP18gm6110020. Taro Sakamaki was supported by the JSPS Core-to-Core Program, JSPS KAKENHI Grant Numbers JP21K20669, JP22K16334, RIKEN Junior Research Associate Program. Katsuyuki Nishi was supported by JSPS Grant Numbers KAKENHI JP18J13408 and 23K15326.

Authorship Contributions

K.N. conceived, performed, analyzed the experiments. T.S. and K.S. performed transplantation experiments. M.M. conceived, performed, analyzed, and oversaw the experiments. K.N. and M.M. wrote the manuscript. T.S., A.N., K.S.K., K.S., M.A., N.Y., and A.T. provided comments on the manuscript.

Disclosure of Conflicts of Interest

The authors declare no conflicts of interest in relation to the present study.

References

Baron, Frédéric, Barry Storer, Michael B. Maris, Jan Storek, Fanny Piette, Monja Metcalf, Kristen White, et al. 2006. “Unrelated Donor Status and High Donor Age Independently Affect Immunologic Recovery after Nonmyeloablative Conditioning.” *Biology of Blood and Marrow Transplantation* 12 (11): 1176–87. https://doi.org/10.1016/j.bbmt.2006.07.004.

Beerman, Isabel, Deepta Bhattacharya, Sasan Zandi, Mikael Sigvardsson, Irving L. Weissman, David Brydere, and Derrick J. Rossia. 2010. “Functionally Distinct Hematopoietic Stem Cells Modulate Hematopoietic Lineage Potential during

569 Aging by a Mechanism of Clonal Expansion." *Proceedings of the National*
570 *Academy of Sciences of the United States of America* 107 (12): 5465–70.
571 https://doi.org/10.1073/pnas.1000834107.
572 Berger, Massimo, O. Figari, B. Bruno, A. Raiola, A. Dominietto, M. Fiorone, M.
573 Podesta, et al. 2008. "Lymphocyte Subsets Recovery Following Allogeneic Bone
574 Marrow Transplantation (BMT): CD4+ Cell Count and Transplant-Related
575 Mortality." *Bone Marrow Transplantation* 41 (1): 55–62.
576 https://doi.org/10.1038/sj.bmt.1705870.
577 Busch, Katrin, Kay Klapproth, Melania Barile, Michael Flossdorf, Tim Holland-Letz,
578 Susan M. Schlenner, Michael Reth, Thomas Höfer, and Hans Reimer Rodewald.
579 2015. "Fundamental Properties of Unperturbed Haematopoiesis from Stem Cells in
580 Vivo." *Nature* 518 (7540): 542–46. https://doi.org/10.1038/nature14242.
581 Challen, Grant A., Nathan C. Boles, Stuart M. Chambers, and Margaret A. Goodell.
582 2010. "Distinct Hematopoietic Stem Cell Subtypes Are Differentially Regulated by
583 TGF-B1." *Cell Stem Cell* 6 (3): 265–78.
584 https://doi.org/10.1016/j.stem.2010.02.002.
585 Chambers, Stuart M., Nathan C. Boles, Kuan Yin K. Lin, Megan P. Tierney, Teresa V.
586 Bowman, Steven B. Bradfute, Alice J. Chen, et al. 2007. "Hematopoietic
587 Fingerprints: An Expression Database of Stem Cells and Their Progeny." *Cell*
588 *Stem Cell* 1 (5): 578–91. https://doi.org/10.1016/j.stem.2007.10.003.
589 Chen, James Y., Masanori Miyanishi, Sean K. Wang, Satoshi Yamazaki, Rahul Sinha,
590 Kevin S. Kao, Jun Seita, Debashis Sahoo, Hiromitsu Nakauchi, and Irving L.
591 Weissman. 2016. "Hoxb5 Marks Long-Term Haematopoietic Stem Cells and
592 Reveals a Homogenous Perivascular Niche." *Nature* 530 (7589): 223–27.
593 https://doi.org/10.1038/nature16943.
594 Cho, Rebecca H., Hans B. Sieburg, and Christa E. Muller-Sieburg. 2008. "A New
595 Mechanism for the Aging of Hematopoietic Stem Cells: Aging Changes the Clonal
596 Composition of the Stem Cell Compartment but Not Individual Stem Cells." *Blood*
597 111 (12): 5553–61. https://doi.org/10.1182/blood-2007-11-123547.
598 Crooke, Stephen N., Inna G. Ovsyannikova, Gregory A. Poland, and Richard B.
599 Kennedy. 2019. "Immunosenescence and Human Vaccine Immune Responses."
600 *Immunity & Ageing* 16 (1): 1–16. https://doi.org/10.1186/s12979-019-0164-9.
601 Dorshkind, Kenneth, Thomas Höfer, Encarnacion Montecino-Rodriguez, Peter D. Pioli,
602 and Hans Reimer Rodewald. 2020. "Do Haematopoietic Stem Cells Age?" *Nature*
603 *Reviews Immunology* 20 (3): 196–202. https://doi.org/10.1038/s41577-019-0236-2.
604 Dykstra, Brad, Sandra Olthof, Jaring Schreuder, Martha Ritsema, and Gerald de Haan.
605 2011. "Clonal Analysis Reveals Multiple Functional Defects of Aged Murine
606 Hematopoietic Stem Cells." *The Journal of Experimental Medicine* 208 (13):
607 2691–2703. https://doi.org/10.1084/jem.20111490.
608 Dykstra, Brad, Sandra Olthof, Jaring Schreuder, Martha Ritsema, and Gerald De Haan.
609 2011. "Clonal Analysis Reveals Multiple Functional Defects of Aged Murine
610 Hematopoietic Stem Cells." *Journal of Experimental Medicine* 208 (13): 2691–
611 2703. https://doi.org/10.1084/jem.20111490.
612 Ergen, Aysegul V., Nathan C. Boles, and Margaret A. Goodell. 2012. "Rantes/Ccl5
613 Influences Hematopoietic Stem Cell Subtypes and Causes Myeloid Skewing."
614 *Blood* 119 (11): 2500–2509. https://doi.org/10.1182/blood-2011-11-391730.

615 Flohr Svendsen, Arthur, Daozheng Yang, Kyung Mok Kim, Seka Lazare, Natalia
616 Skinder, Erik Zwart, Anna Mura-Meszaros, et al. 2021. “A Comprehensive
617 Transcriptome Signature of Murine Hematopoietic Stem Cell Aging.” *Blood* 138
618 (6): 439–51. https://doi.org/10.1182/blood.2020009729.
619 Geiger, Hartmut, Gerald De Haan, and M. Carolina Florian. 2013. “The Ageing
620 Haematopoietic Stem Cell Compartment.” *Nature Reviews Immunology* 13 (5):
621 376–89. https://doi.org/10.1038/nri3433.
622 González-Vicent, Marta, Blanca Molina, Natalia Deltoro, Julián Sevilla, José Luis
623 Vicario, Ana Castillo, Manuel Ramirez, and Miguel Ángel Díaz. 2017. “Donor
624 Age Matters in T-Cell Depleted Haploidentical Hematopoietic Stem Cell
625 Transplantation in Pediatric Patients: Faster Immune Reconstitution Using
626 Younger Donors.” *Leukemia Research* 57: 60–64.
627 https://doi.org/10.1016/j.leukres.2017.03.001.
628 Grover, Amit, Alejandra Sanjuan-Pla, Supat Thongjuea, Joana Carrelha, Alice
629 Giustacchini, Adriana Gambardella, Iain Macaulay, et al. 2016. “Single-Cell RNA
630 Sequencing Reveals Molecular and Functional Platelet Bias of Aged
631 Haematopoietic Stem Cells.” *Nature Communications* 7.
632 https://doi.org/10.1038/ncomms11075.
633 Haan, Gerald de, and Seka Simone Lazare. 2018. “Aging of Hematopoietic Stem Cells.”
634 *Blood* 131 (5): 479–87. https://doi.org/10.1182/blood-2017-06-746412.
635 Haan, Gerald De, and Seka Simone Lazare. 2018. “Aging of Hematopoietic Stem
636 Cells.” www.bloodjournal.org.
637 Jones, D. Leanne, and Thomas A. Rando. 2011. “Emerging Models and Paradigms for
638 Stem Cell Ageing.” *Nature Cell Biology* 13 (5): 506–12.
639 https://doi.org/10.1038/ncb0511-506.
640 Kim, Daehwan, Ben Langmead, and Steven L. Salzberg. 2015. “HISAT: A Fast Spliced
641 Aligner with Low Memory Requirements.” *Nature Methods* 12 (4): 357–60.
642 https://doi.org/10.1038/nmeth.3317.
643 Kowalczyk, Monika S., Itay Tirosh, Dirk Heckl, Tata Nageswara Rao, Atray Dixit,
644 Brian J. Haas, Rebekka K. Schneider, Amy J. Wagers, Benjamin L. Ebert, and
645 Aviv Regev. 2015. “Single-Cell RNA-Seq Reveals Changes in Cell Cycle and
646 Differentiation Programs upon Aging of Hematopoietic Stem Cells.” *Genome*
647 *Research* 25 (12): 1860–72. https://doi.org/10.1101/gr.192237.115.
648 Liberzon, Arthur, Chet Birger, Helga Thorvaldsdóttir, Mahmoud Ghandi, Jill P.
649 Mesirov, and Pablo Tamayo. 2015. “The Molecular Signatures Database Hallmark
650 Gene Set Collection.” *Cell Systems* 1 (6): 417–25.
651 https://doi.org/10.1016/j.cels.2015.12.004.
652 Maas, Nicolaas G. van der, Erik G.J. von Asmuth, Dagmar Berghuis, Pauline A. van
653 Schouwenburg, Hein Putter, Mirjam van der Burg, and Arjan C. Lankester. 2021.
654 “Modeling Influencing Factors in B-Cell Reconstitution After Hematopoietic Stem
655 Cell Transplantation in Children.” *Frontiers in Immunology* 12 (May): 1–8.
656 https://doi.org/10.3389/fimmu.2021.684147.
657 Majeti, Ravindra, Christopher Y. Park, and Irving L. Weissman. 2007. “Identification of
658 a Hierarchy of Multipotent Hematopoietic Progenitors in Human Cord Blood.”
659 *Cell Stem Cell* 1 (6): 635–45. https://doi.org/10.1016/j.stem.2007.10.001.
660 Mann, Mati, Arnav Mehta, Carl G de Boer, Monika S Kowalczyk, Kevin Lee, Pearce
661 Haldeman, Noga Rogel, et al. 2018. “Heterogeneous Responses of Hematopoietic

662 Stem Cells to Inflammatory Stimuli Are Altered with Age." *Cell Reports* 25 (11):
663 2992–3005. https://doi.org/10.1016/j.celrep.2018.11.056.
664 Mejia-Ramirez, Eva, and Maria Carolina Florian. 2020. "Understanding Intrinsic
665 Hematopoietic Stem Cell Aging." *Haematologica* 105 (1): 22–37.
666 https://doi.org/10.3324/haematol.2018.211342.
667 Min, Hyeyoung, Encarnacion Montecino-Rodriguez, and Kenneth Dorshkind. 2006.
668 "Effects of Aging on the Common Lymphoid Progenitor to Pro-B Cell Transition."
669 *The Journal of Immunology* 176 (2): 1007–12.
670 https://doi.org/10.4049/jimmunol.176.2.1007.
671 Montecino-Rodriguez, Encarnacion, Ying Kong, David Casero, Adrien Rouault,
672 Kenneth Dorshkind, and Peter D. Pioli. 2019. "Lymphoid-Biased Hematopoietic
673 Stem Cells Are Maintained with Age and Efficiently Generate Lymphoid
674 Progeny." *Stem Cell Reports* 12 (3): 584–96.
675 https://doi.org/10.1016/j.stemcr.2019.01.016.
676 Morrison, Sean J., and Irving L. Weissman. 1994. "The Long-Term Repopulating
677 Subset of Hematopoietic Stem Cells Is Deterministic and Isolatable by
678 Phenotype." *Immunity* 1 (8): 661–73. https://doi.org/10.1016/1074-
679 7613(94)90037-X.
680 Morrison, Sean J, A M Wandycz, K Akashi, A Globerson, and Irving L Weissman.
681 1996. "The Aging of Hematopoietic Stem Cells." *Nature Medicine* 2 (9): 1011–16.
682 https://doi.org/10.1038/nm0996-1011.
683 Muller-Sieburg, Christa E., Rebecca H. Cho, Lars Karlsson, Jing F. Huang, and Hans B.
684 Sieburg. 2004. "Myeloid-Biased Hematopoietic Stem Cells Have Extensive Self-
685 Renewal Capacity but Generate Diminished Lymphoid Progeny with Impaired IL-
686 7 Responsiveness." *Blood* 103 (11): 4111–18. https://doi.org/10.1182/blood-2003-
687 10-3448.
688 Nilsson, Alexandra Rundberg, Shamit Soneji, Sofia Adolfsson, David Bryder, and
689 Cornelis Jan Pronk. 2016. "Human and Murine Hematopoietic Stem Cell Aging Is
690 Associated with Functional Impairments and Intrinsic Megakaryocytic/Erythroid
691 Bias." *PLoS ONE* 11 (7): 1–20. https://doi.org/10.1371/journal.pone.0158369.
692 Nishi, Katsuyuki, Taro Sakamaki, Kay Sadaoka, Momo Fujii, Akifumi Takaori-Kondo,
693 James Y. Chen, and Masanori Miyanishi. 2022. "Identification of the Minimum
694 Requirements for Successful Haematopoietic Stem Cell Transplantation." *British*
695 *Journal of Haematology* 196 (3): 711–23. https://doi.org/10.1111/bjh.17867.
696 Pang, Wendy W., Elizabeth A. Price, Debashis Sahoo, Isabel Beerman, William J.
697 Maloney, Derrick J. Rossi, Stanley L. Schrier, and Irving L. Weissman. 2011.
698 "Human Bone Marrow Hematopoietic Stem Cells Are Increased in Frequency and
699 Myeloid-Biased with Age." *Proceedings of the National Academy of Sciences of*
700 *the United States of America* 108 (50): 20012–17.
701 https://doi.org/10.1073/pnas.1116110108.
702 Pertea, Mihaela, Daehwan Kim, Geo M. Pertea, Jeffrey T. Leek, and Steven L.
703 Salzberg. 2016. "Transcript-Level Expression Analysis of RNA-Seq Experiments
704 with HISAT, StringTie and Ballgown." *Nature Protocols* 11 (9): 1650–67.
705 https://doi.org/10.1038/nprot.2016.095.
706 Pietras, Eric M. 2017. "Inflammation: A Key Regulator of Hematopoietic Stem Cell
707 Fate in Health and Disease." *Blood* 130 (15): 1693–98.
708 https://doi.org/10.1182/blood-2017-06-780882.

Pinho, Sandra, Tony Marchand, Eva Yang, Qiaozhi Wei, Claus Nerlov, and Paul S. Frenette. 2018. "Lineage-Biased Hematopoietic Stem Cells Are Regulated by Distinct Niches." *Developmental Cell* 44 (5): 634-641.e4. https://doi.org/10.1016/j.devcel.2018.01.016.

Pronk, Cornelis J.H., Derrick J. Rossi, Robert Månsson, Joanne L. Attema, Gudmundur Logi Norddahl, Charles Kwok Fai Chan, Mikael Sigvardsson, Irving L. Weissman, and David Bryder. 2007. "Elucidation of the Phenotypic, Functional, and Molecular Topography of a Myeloerythroid Progenitor Cell Hierarchy." *Cell Stem Cell* 1 (4): 428–42. https://doi.org/10.1016/j.stem.2007.07.005.

Robinson, Mark D., Davis J. McCarthy, and Gordon K. Smyth. 2009. "EdgeR: A Bioconductor Package for Differential Expression Analysis of Digital Gene Expression Data." *Bioinformatics* 26 (1): 139–40. https://doi.org/10.1093/bioinformatics/btp616.

Rossi, Derrick J., David Bryder, Jun Seita, Andre Nussenzweig, Jan Hoeijmakers, and Irving L. Weissman. 2007. "Deficiencies in DNA Damage Repair Limit the Function of Haematopoietic Stem Cells with Age." *Nature* 447 (7145): 725–29. https://doi.org/10.1038/nature05862.

Rossi, Derrick J., Catriona H.M. Jamieson, and Irving L. Weissman. 2008. "Stems Cells and the Pathways to Aging and Cancer." *Cell* 132 (4): 681–96. https://doi.org/10.1016/j.cell.2008.01.036.

Rossi, Derrick J, David Bryder, Jacob M Zahn, Henrik Ahlenius, Rebecca Sonu, Amy J Wagers, and Irving L Weissman. 2005. "Cell Intrinsic Alterations Underlie Hematopoietic Stem Cell Aging." *Proceedings of the National Academy of Sciences of the United States of America* 102 (26): 9194–99. https://doi.org/10.1073/pnas.0503280102.

Rossi, Simona W., Lukas T. Jeker, Tomoo Ueno, Sachiyo Kuse, Marcel P. Keller, Saulius Zuklys, Andrei V. Gudkov, et al. 2007. "Keratinocyte Growth Factor (KGF) Enhances Postnatal T-Cell Development via Enhancements in Proliferation and Function of Thymic Epithelial Cells." *Blood* 109 (9): 3803–11. https://doi.org/10.1182/blood-2006-10-049767.

Sakamaki, Taro, Kevin S. Kao, Katsuyuki Nishi, James Y. Chen, Kay Sadaoka, Momo Fujii, Akifumi Takaori-Kondo, Irving L. Weissman, and Masanori Miyanishi. 2021. "Hoxb5 Defines the Heterogeneity of Self-Renewal Capacity in the Hematopoietic Stem Cell Compartment." *Biochemical and Biophysical Research Communications* 539 (February): 34–41. https://doi.org/10.1016/j.bbrc.2020.12.077.

Sanjuan-Pla, Alejandra, Iain C. Macaulay, Christina T. Jensen, Petter S. Woll, Tiago C. Luis, Adam Mead, Susan Moore, et al. 2013. "Platelet-Biased Stem Cells Reside at the Apex of the Haematopoietic Stem-Cell Hierarchy." *Nature* 502 (7470): 232–36. https://doi.org/10.1038/nature12495.

SanMiguel, Jennifer M., Kira Young, and Jennifer J. Trowbridge. 2020. "Hand in Hand: Intrinsic and Extrinsic Drivers of Aging and Clonal Hematopoiesis." *Experimental Hematology* 91: 1–9. https://doi.org/10.1016/j.exphem.2020.09.197.

Schultz, Michael B., and David A. Sinclair. 2016. "When Stem Cells Grow Old: Phenotypes and Mechanisms of Stem Cell Aging." *Development (Cambridge)* 143 (1): 3–14. https://doi.org/10.1242/dev.130633.

Spangrude, Gerald J., Diane M. Brooks, and Daniel B. Tumas. 1995. "Long-Term Repopulation of Irradiated Mice with Limiting Numbers of Purified Hematopoietic Stem Cells: In Vivo Expansion of Stem Cell Phenotype but Not Function." *Blood* 85 (4): 1006–16. https://doi.org/10.1182/blood.v85.4.1006.bloodjournal8541006.

Spangrude, Gerald J, Shelly Heimfeld, and Irving L Weissman. 1988. "Purification and Characterization of Mouse Hematopoietic Stem Cells." *Science (New York, N.Y.)* 241 (4861): 58–62. https://doi.org/10.1126/science.2898810.

Subramanian, Aravind, Pablo Tamayo, Vamsi K. Mootha, Sayan Mukherjee, Benjamin L. Ebert, Michael A. Gillette, Amanda Paulovich, et al. 2005. "Gene Set Enrichment Analysis: A Knowledge-Based Approach for Interpreting Genome-Wide Expression Profiles." *Proceedings of the National Academy of Sciences of the United States of America* 102 (43): 15545–50. https://doi.org/10.1073/pnas.0506580102.

Sudo, K, H Ema, Y Morita, and H Nakauchi. 2000. "Age-Associated Characteristics of Murine Hematopoietic Stem Cells [In Process Citation]." *J Exp Med* 192 (9): 1273–80.

Webster, Robert G. 2000. "Immunity to Influenza in the Elderly." *Vaccine* 18 (16): 1686–89. https://doi.org/10.1016/S0264-410X(99)00507-1.

Weissman, Irving L., and Judith A. Shizuru. 2008. "The Origins of the Identification and Isolation of Hematopoietic Stem Cells, and Their Capability to Induce Donor-Specific Transplantation Tolerance and Treat Autoimmune Diseases." *Blood* 112 (9): 3543–53. https://doi.org/10.1182/blood-2008-08-078220.

Figure 1.

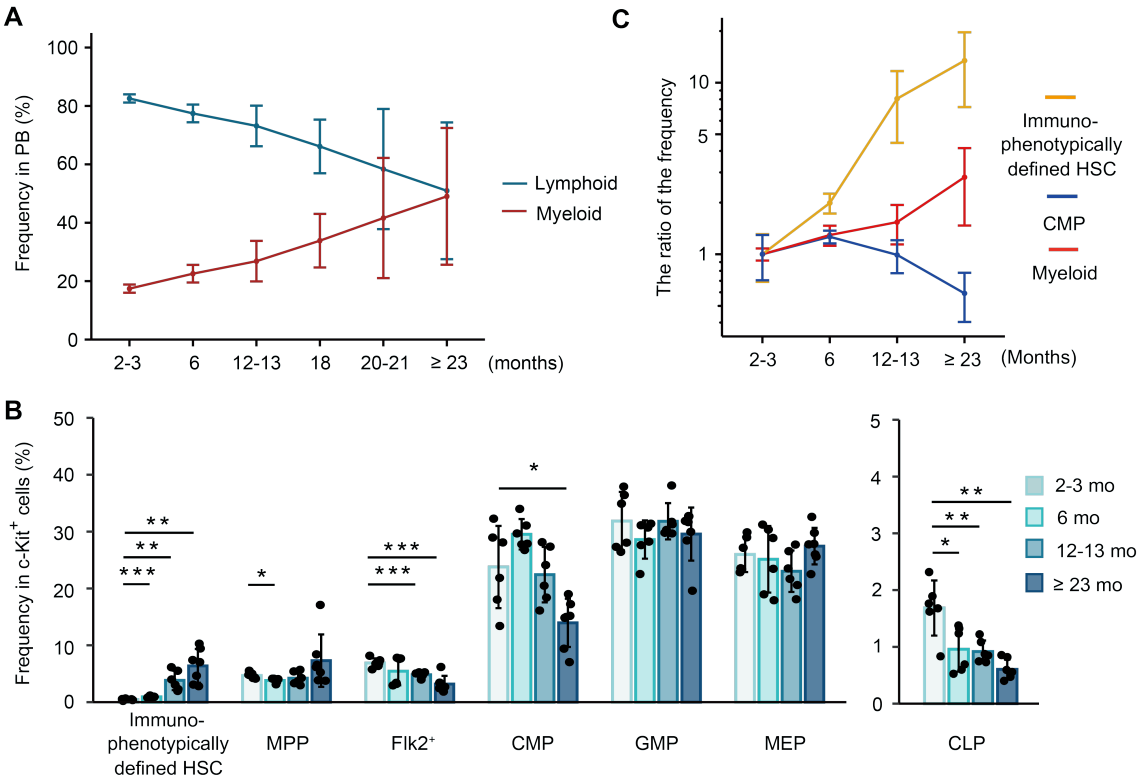

Figure 1. Comprehensive analysis of hematopoietic alternations with age shows a discrepancy of age-associated changes between peripheral blood and bone marrow

(A) Average frequency of myeloid cells (neutrophils, monocytes) and lymphoid cells (B cells, T cells, and NK cells) in PB at the age of 2-3 months (n = 6), 6 months (n = 6), 12-13 months (n = 6), 18 months (n = 6), 20-21 months (n = 5), ≥ 23 months (n = 16). Abbreviation: PB = Peripheral blood.

(B) Average frequency of immunophenotypically defined HSC and progenitor cells in BM of 2-3-month mice (n = 6), 6-month mice (n = 6), 12-13-month mice (n = 6), ≥ 23-month mice (n = 7).

(C) Age-associated changes of immunophenotypically defined HSC and myeloid differentiation components (CMP and myeloid cells in the PB). The ratio of aged to young

814 frequency was calculated as (the fraction frequency at each aged mice (%)) / (the average
815 fraction frequency at 2-3-month mice (%)). *$P < 0.05$. **$P < 0.01$. ***$P < 0.001$. Data
816 and error bars represent means ± standard deviation.
817
818
819
820
821
822
823
824
825
826
827
828
829
830
831
832
833
834
835
836
837

Figure 2.

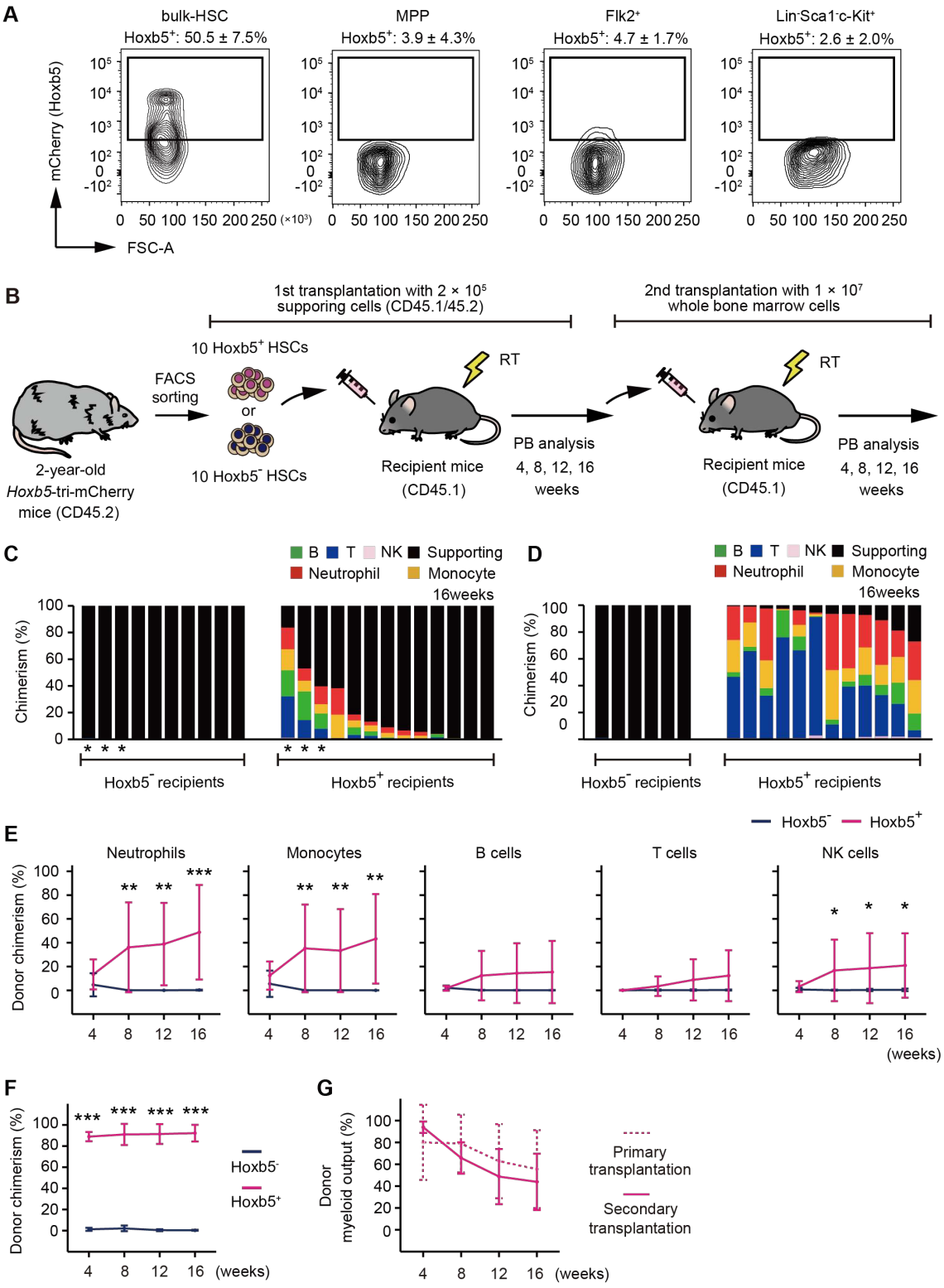

Figure 2. The expansion of myeloid-biased clones was not observed in 2-year-old LT-HSCs after their transplantation.

(A) Hoxb5 reporter expression in bulk-HSC, MPP, Flk2$^+$, and Lin$^-$Sca1$^-$c-Kit$^+$ populations in the 2-year-old *Hoxb5*-tri-mCherry mice. Values indicate the percentage of mCherry$^+$ cells ± standard deviation in each fraction (n = 3).

(B) Experimental design to assess the long-term reconstitution ability of Hoxb5$^+$ HSCs or Hoxb5$^-$ HSCs. Hoxb5$^+$ HSCs and Hoxb5$^-$ HSCs were isolated from 2-year-old CD45.2 *Hoxb5*-tri-mCherry mice and were transplanted into lethally irradiated CD45.1 recipient mice with 2 × 10^5 supporting cells (Hoxb5$^+$ HSCs, n = 13; Hoxb5$^-$ HSCs, n = 10). For secondary transplants, 1 × 10^7 whole BM cells were transferred from primary recipient mice. Abbreviations: PB = Peripheral blood, RT = Radiation therapy.

(C) Percentage chimerism at 16 weeks after receiving ten aged Hoxb5$^-$ HSCs or ten aged Hoxb5$^+$ HSCs. Each column represents an individual mouse.

(D) Percentage chimerism at 16 weeks after whole BM secondary transplantation. Donor whole BM cells for secondary transplantation were taken from mice denoted by * in Figure 2C.

(E) Kinetics of average donor chimerism in each PB fraction after primary transplantation.

(F) Kinetics of average donor chimerism after secondary transplantation.

(G) Kinetics of average donor myeloid output (myeloid proportion in donor cells) in LT-HSC recipient mice after primary and secondary transplantation. *P < 0.05. **P < 0.01. ***P < 0.001. Data and error bars represent means ± standard deviation.

Figure 3.

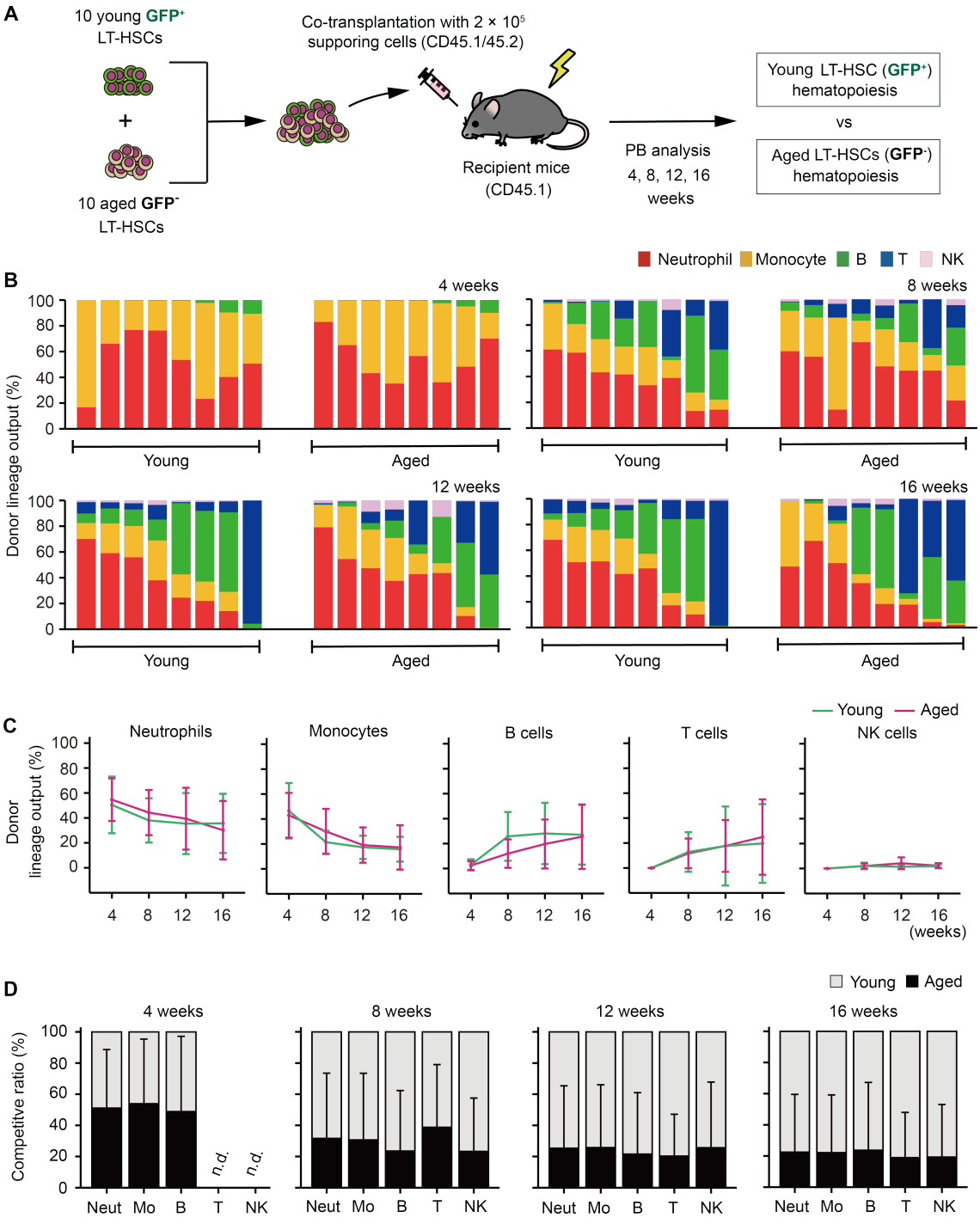

Figure 3. Aged LT-HSCs show balanced hematopoiesis throughout life

908 (A) Experimental design for competitive co-transplantation assay using young LT-HSCs
909 sorted from *Hoxb5*-tri-mCherry GFP mice and aged LT-HSCs sorted from *Hoxb5*-tri-
910 mCherry mice. Ten CD45.2$^+$ young LT-HSCs and ten CD45.2$^+$ aged LT-HSCs were
911 transplanted with 2 × 10^5 CD45.1$^+$/CD45.2$^+$ supporting cells into lethally irradiated
912 CD45.1$^+$ recipient mice (n = 8).
913 (B) Lineage output of young or aged LT-HSCs at 4, 8, 12, 16 weeks after transplantation.
914 Each bar represents an individual mouse.
915 (C) Lineage output kinetics of young LT- HSCs or aged LT- HSCs at 4, 8, 12, 16 weeks
916 post-transplant.
917 (D) Competitive analysis of young LT-HSCs vs. aged LT-HSCs lineage output at 4, 8,
918 12, 16 weeks post-transplant. Competitive ratio was calculated as the proportion of young
919 LT-HSCs derived cells vs. aged LT- HSCs derived cells in each fraction. Abbreviations:
920 Neut = Neutrophils, Mo = Monocytes, B = B cells, T = T cells, and NK = NK cells. Data
921 and error bars represent means ± standard deviation. “n.d.” stands for “not detected.”
922
923
924
925
926
927
928
929
930
931

Figure 4.

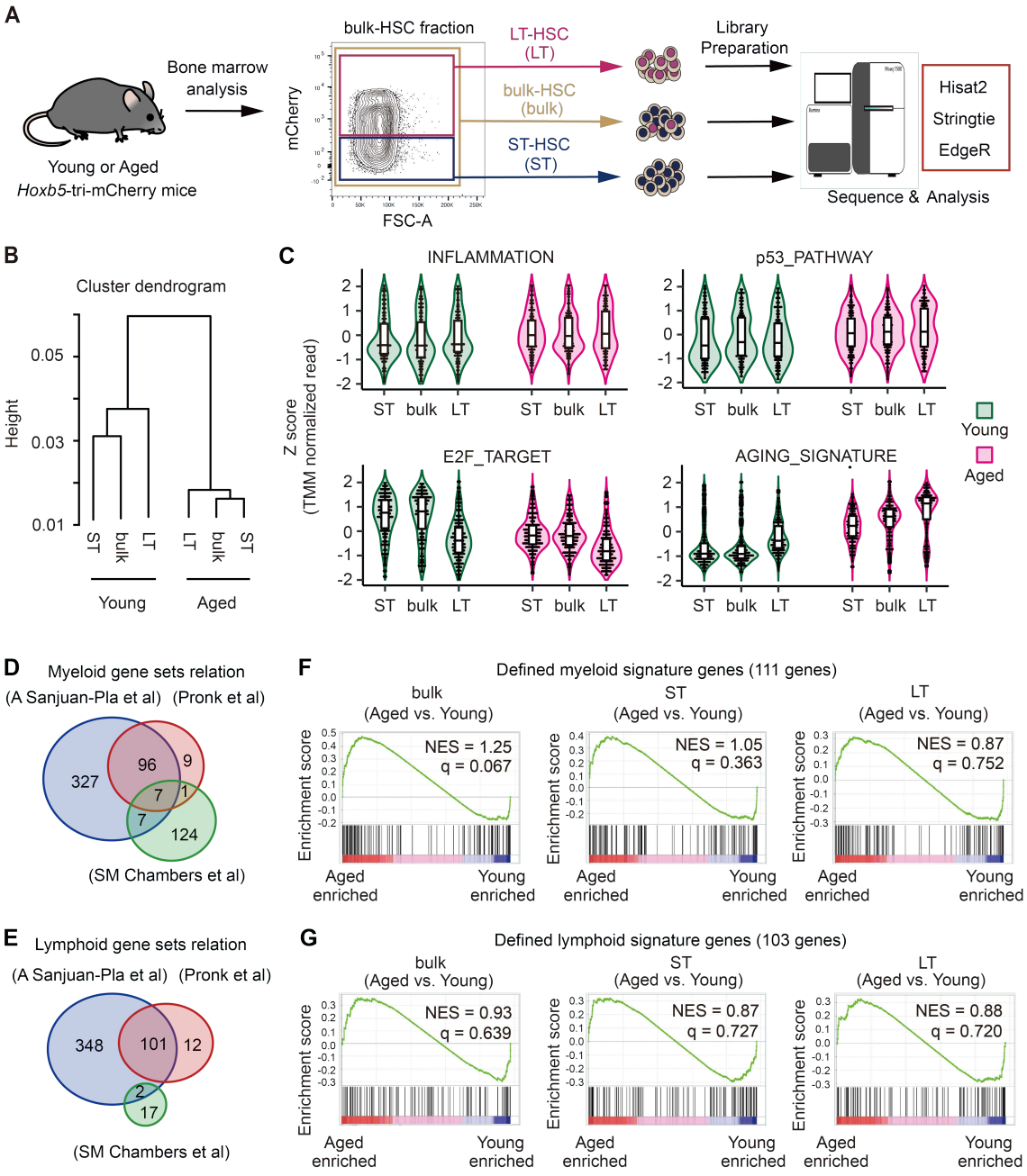

Figure 4. Myeloid-associated genes were not enriched in aged LT-HSCs compared to their young counterparts

(A) Experimental schematic for transcriptome analysis. LT-HSCs (n = 3), ST-HSCs (n = 3), and bulk-HSCs (n = 3) were sorted from young (2-3 months) or aged (23-25 months) *Hoxb5*-tri-mCherry mice, after which each RNA was harvested for RNA sequencing.

(B) Hierarchical clustering dendrogram of whole transcriptomes using Spearman distance and the Ward clustering algorithm.

(C) Violin plots showing normalized gene expression levels for each gene set in young and aged LT-HSCs, ST-HSCs, and bulk-HSCs. Expression values for each gene were standardized independently by applying *Z* score transformation.

(D, E) Venn diagram showing the overlap of genes between three myeloid signature gene sets, and lymphoid signature gene sets (A Sanjuan-Pla et al., 2013, Pronk et al., 2007, SM Chambers et al., 2007).

(F, G) Signature enrichment plots from GSEA analysis using defined myeloid and lymphoid signature gene sets that overlapped in the three gene sets. Values indicated on individual plots are the normalized Enrichment Score (NES) and q-value of enrichment.

Figure 5.

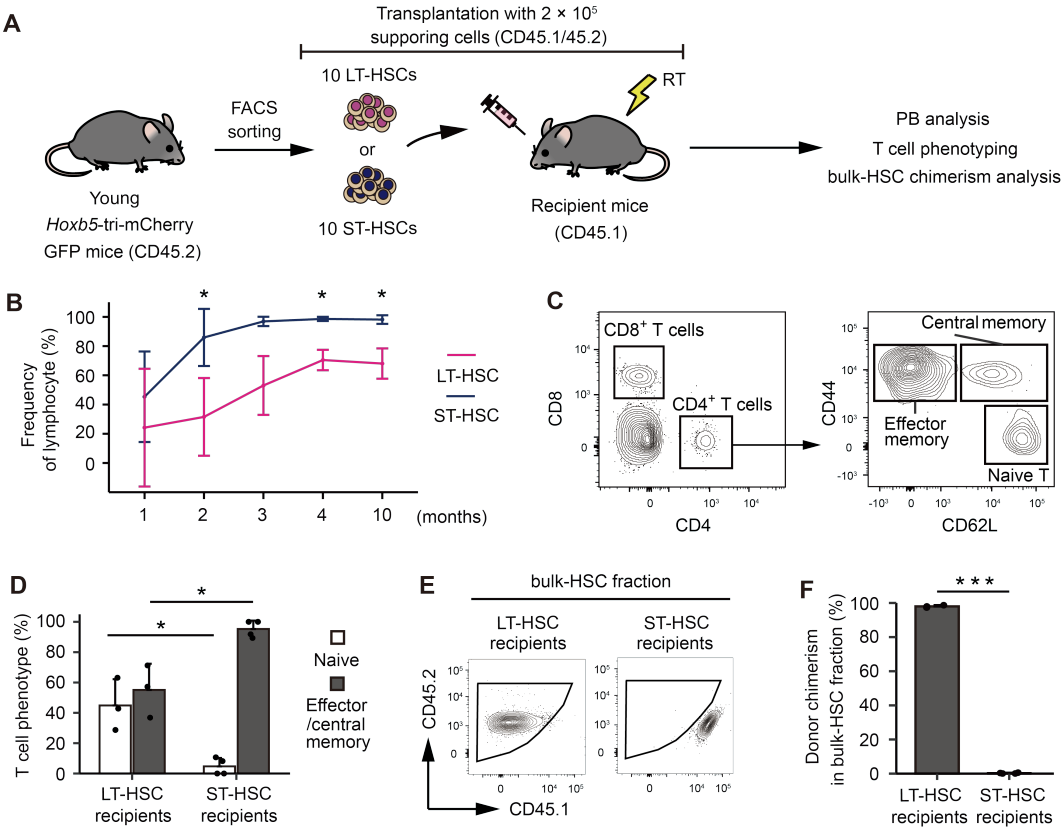

Figure 5. The memory-type lymphocytes in the peripheral blood make it look as if ST-HSCs are lymphoid-biased HSCs

(A) Experimental design for assessing the lineage output of young LT-HSCs or ST-HSCs. Ten LT-HSCs, or ten ST-HSCs were isolated from 2-month-old CD45.2 *Hoxb5*-tri-mCherry GFP mice and were transplanted into lethally irradiated CD45.1 recipient mice with 2×10^5 supporting cells (LT-HSCs, $n = 3$; ST-HSCs, $n = 4$).

(B) Kinetics of average frequency of lymphoid cells (B cells, T cells, and NK cells) in donor fraction after LT-HSCs or ST-HSCs transplantation.

(C) Gating scheme to identify memory (Central and effector) T cells and naive T cells in the PB after excluding doublets, dead cells, and non-donor cells.

(D) Percentage of memory (Central and effector) T cells and naive T cells in donor $CD4^+$ fraction 10 months after LT-HSC or ST-HSC transplantation.

(E) Gating scheme to identify donor cells in bulk-HSC fraction in bone marrow analysis.

(F) Donor chimerism in bulk-HSC fraction 12 months after LT-HSCs or ST-HSCs transplantation. *$P < 0.05$. ***$P < 0.001$. Data and error bars represent means ± standard deviation.

Figure 6.

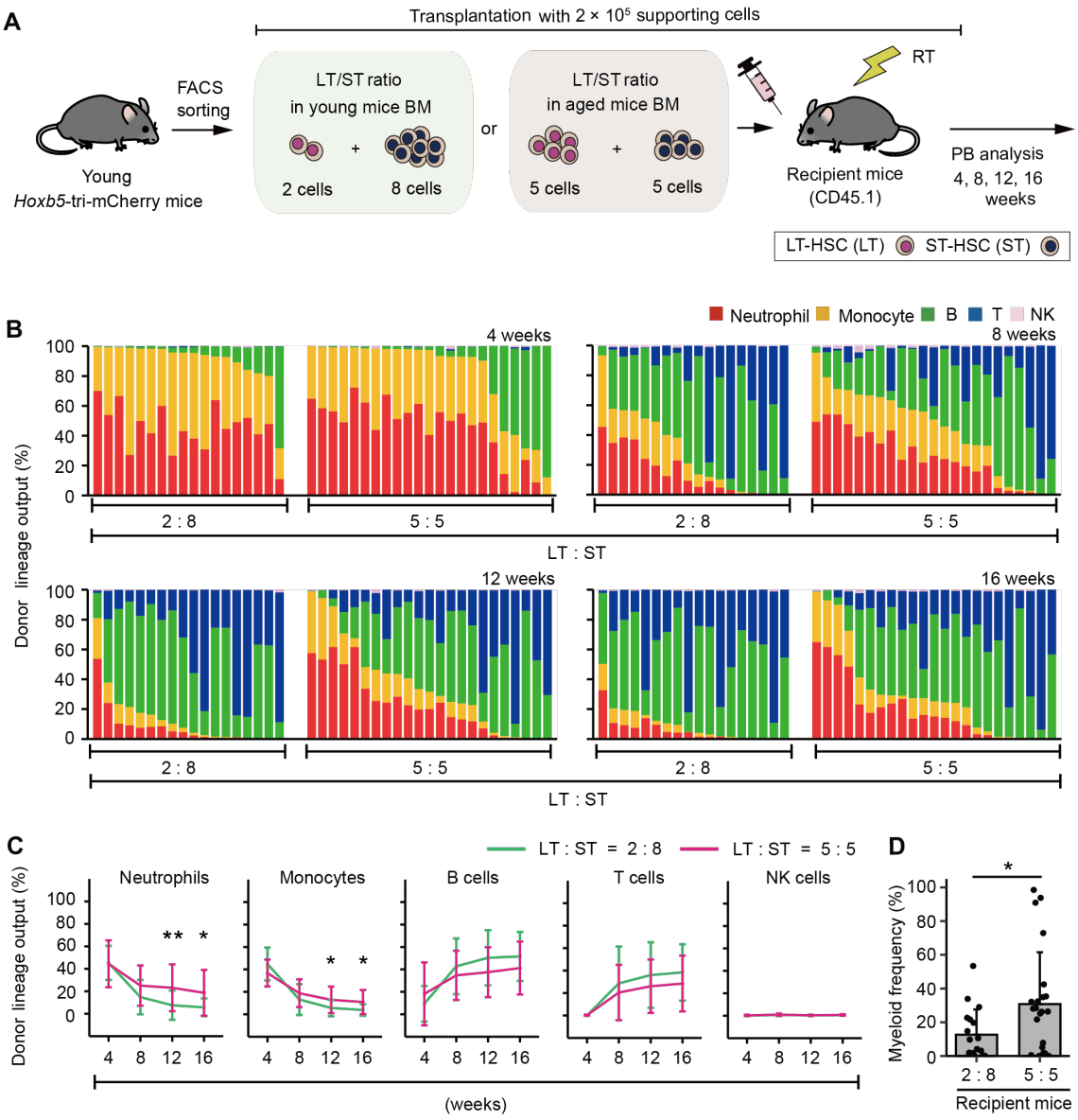

Figure 6. Hematopoiesis after transplantation inclined either toward myeloid or lymphoid cell production by artificially changing the ratio of LT-HSC/ST-HSC

(A) Experimental design for the transplantation of 2-3-month-old LT-HSCs and ST-HSCs in a 2:8 ratio (the same ratio as in young mice BM) or 5:5 ratio (the same ratio as in aged mice BM). Donor cells were transplanted with 2 × 10^5 CD45.1$^+$/CD45.2$^+$

supporting cells into lethally irradiated CD45.1^{+} recipient mice (2:8 ratio, n = 18; 5:5 ratio, n = 23).

(B) Donor lineage output of young LT-HSCs and ST-HSCs transplanted either in a 2:8 ratio or a 5:5 ratio at 4, 8, 12, 16 weeks post-transplant. Each bar represents an individual mouse.

(C) Kinetics of average lineage output of young LT-HSCs and ST-HSCs in a 2:8 ratio or a 5:5 ratio at 4, 8, 12, 16 weeks post-transplant.

(D) Frequency of myeloid cells in donor cell fraction. *$P < 0.05$. **$P < 0.01$. Error bars represent standard deviation. Data represent two independent experiments.

Figure 7.

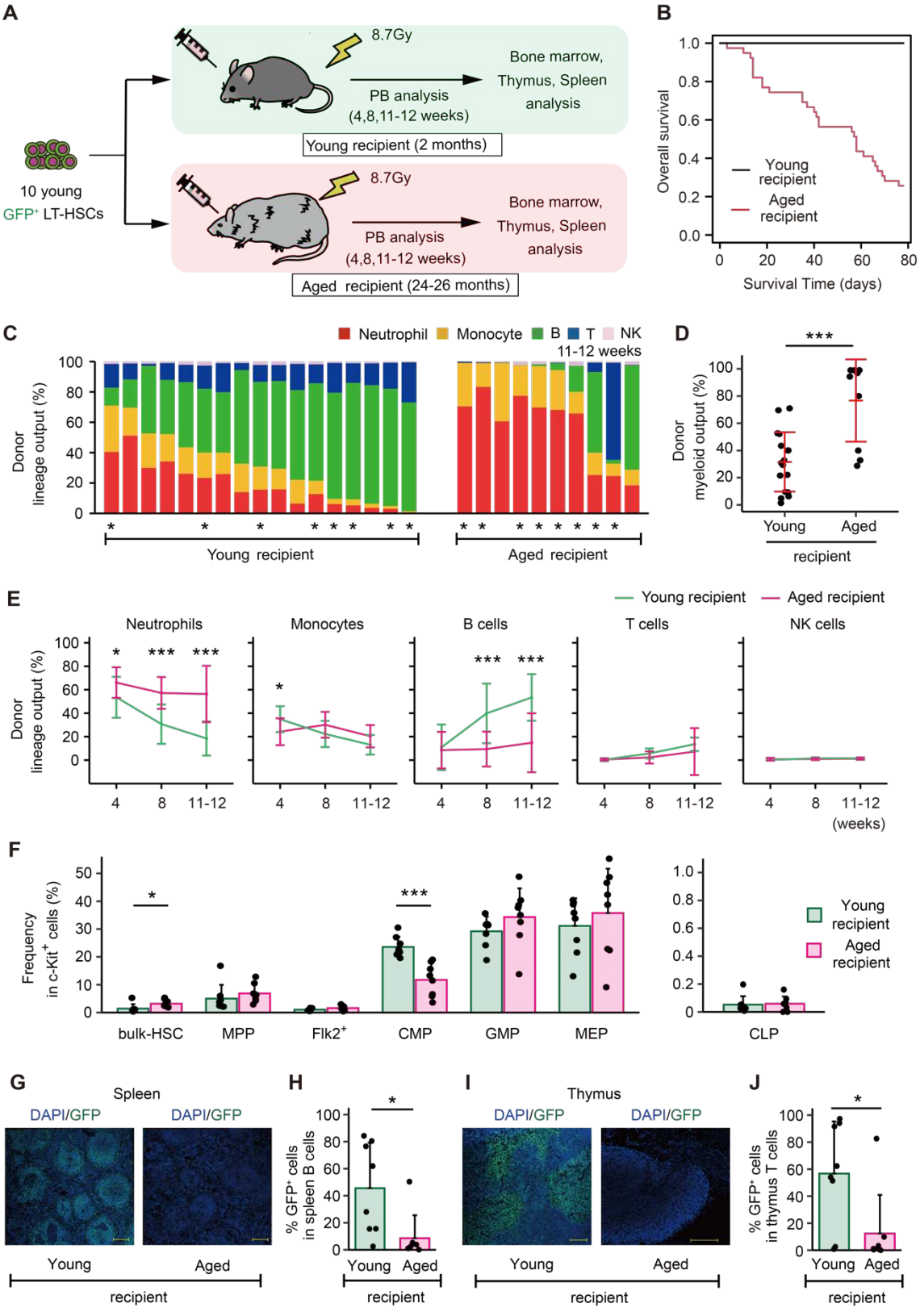

Figure 7. Age-associated physiological changes drive differentiation of LT-HSCs toward myeloid cells

(A) Experimental design for assessing the impact of age-associated physiological changes on differentiation of LT-HSCs. Ten GFP^+ LT-HSCs sorted from young (2-3 months) *Hoxb5*-tri-mCherry GFP mice, were transplanted with 2×10^5 $CD45.1^+/CD45.2^+$ supporting cells into lethally irradiated young or aged recipient mice. We defined donor cells as GFP^+ cells and supporting cells as $CD45.1^+/CD45.2^+$ cells.

(B) Survival rate of recipient mice in each group.

(C) Donor lineage output in young or aged recipient mice 11-12 weeks after transplanting young LT-HSCs (young recipient, $n = 17$; aged recipient, $n = 10$).

(D) Myeloid output (Frequency of donor myeloid cells in donor fraction) in young or aged recipient mice 11-12 weeks after transplantation.

(E) Kinetics of lineage output from donor LT-HSCs in young or aged recipient mice 4, 8, 11-12 weeks after transplantation.

(F) Average frequency of donor bulk-HSC and progenitor cells in donor $c\text{-}Kit^+$ cells in BM (young recipient, $n = 8$; aged recipient, $n = 8$). BM samples were taken from mice denoted by * in Figure 7C.

(G) Representative immunofluorescence images of frozen spleen sections derived from young or aged recipient mice. Green: donor cells (GFP fluorescence); blue: DNA (DAPI); Scale bar: 200 μm.

(H) Frequency of donor cells in spleen B cells of young or aged recipient mice (young recipient, $n = 8$; aged recipient, $n = 8$). Spleens are taken from mice denoted by * in Figure 7C.

(I) Representative immunofluorescence images of frozen thymus sections derived from young or aged recipient mice. Green: donor cells (GFP fluorescence); blue: DNA (DAPI); Scale bar: 200 μm.

(J) Frequency of donor cells in thymus T cells of young or aged recipient mice (young recipient, $n = 8$; aged recipient, $n = 8$). Thymi are taken from mice denoted by * in Figure 7C. $*P < 0.05$. $***P < 0.001$. Error bars represent standard deviation. Data represent two independent experiments.

Figure 8.

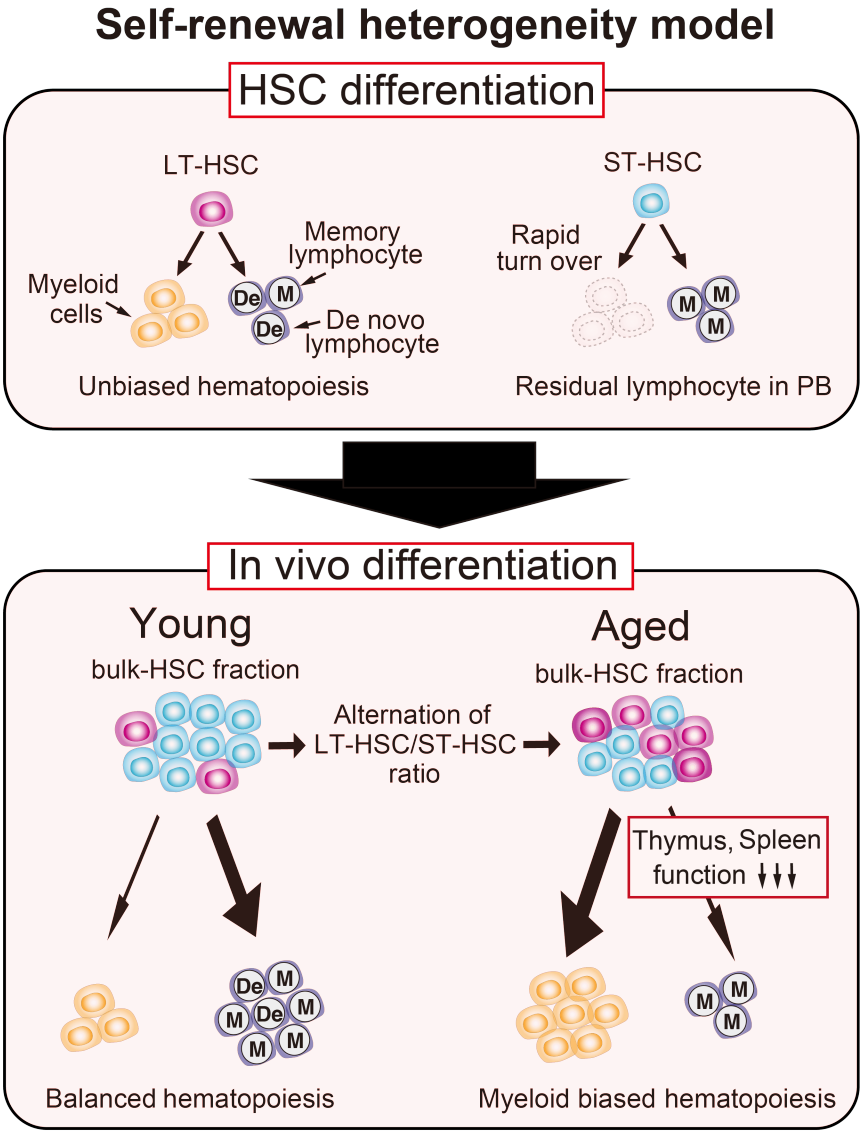

Figure 8. Our new model: **Self-renewal heterogeneity model**. It has been thought that there were myeloid (My-) or lymphoid biased (Ly-) HSCs, and that clonal selection of My-HSCs caused age-associated myeloid biased hematopoiesis. However, in our model, LT-HSCs represent unbiased hematopoiesis throughout life. ST-HSCs lose their hematopoietic ability within a short period and memory-type lymphocytes remains in the PB after ST-HSC transplantation. These remaining memory-type lymphocytes make it

look as if ST-HSCs are lymphoid-biased (The upper section). As a result, the age-associated relative decrease of ST-HSCs in bulk-HSC fraction causes myeloid biased hematopoiesis with age. Additionally, the blockage of lymphoid differentiation at spleen and thymus accelerates further myeloid biased hematopoiesis in aged mice (The lower section).